

Thermally stimulated structural changes in highly oriented glassy poly(ethylene terephthalate)

Ulrich Göschel*

Max-Planck-Institut für Polymerforschung, Postfach 3148, D-55021 Mainz, Germany
(Received 15 January 1996)

Glassy poly(ethylene terephthalate) (PET) structures with an extraordinarily large chain orientation have been prepared from isotropic and X-ray amorphous initial film strips by applying a cold-drawing procedure with well defined parameters. Under annealing conditions, the resulting changes of the supermolecular structure and the thermomechanical behaviour are investigated. Differential scanning calorimetric studies have revealed a starting crystallization of the highly anisotropic and glassy PET structures at temperatures as low as 56°C. *In situ* two-dimensional wide-angle X-ray scattering (WAXS) experiments have been performed to describe the formation of the crystalline order with temperature. Synchrotron WAXS investigations focusing on the (0 1 0), ($\bar{1}$ 1 0) and (1 0 0) reflections show a fast crystallization process. The final crystal structure at each temperature above 120°C is reached within less than 7.5 min. Dynamic mechanical thermal analysis, shrinkage strain and shrinkage stress measurements are discussed with respect to the relaxation of local molecular orientation as well as crystallization processes. Copyright © 1996 Elsevier Science Ltd.

(Keywords: poly(ethylene terephthalate); relaxation; crystallization)

INTRODUCTION

Poly(ethylene terephthalate) (PET) is used in a variety of commercial applications such as films and fibres. In many cases, high mechanical stiffness and strength along with a large dimensional stability are required. Drawing is an essential fabrication process to achieve well-oriented structures with appropriate mechanical properties. Extraordinarily large chain orientations, which are desired to increase the material stiffness, can be obtained by applying a multistep drawing procedure and passing through an oriented and non-crystalline intermediate structure¹.

Glasses usually exist in a non-equilibrium state². Their supermolecular structure is non-crystalline according to wide-angle X-ray scattering (WAXS) investigations and no large-range structure is observed by small-angle X-ray scattering (SAXS). Oriented and glassy structures can be achieved under certain thermomechanical conditions. Temperature and mechanical stress are necessary for the orientation process, but these parameters also initiate crystallization and relaxation of chain segments. Relaxation processes lead to a decrease in the molecular orientation.

Drawing experiments on PET revealed that temperatures either below or close to the glass transition (T_g) are essential to achieve glassy structures with a large chain orientation^{1,3–5}. In general, the drawing temperature, stress and rate of drawing should be small to avoid crystallization^{1,3,6,7}.

It is well-known that oriented and glassy PET structures change their supermolecular structure easily during annealing and mechanical loading. Major processes are both the crystallization and the orientation relaxation. The crystallization process in oriented PET was investigated by several authors^{8–13}. Biangardi and Zachmann⁸ found that the PET structure obtained after crystallization depends mainly on the birefringence after stretching but before crystallization. According to Le Bourvellec *et al.*⁹, the kinetics of the crystallization is controlled by the initial orientation and the annealing temperature. The half-time of the strain-induced crystallization is much smaller than that of isothermal crystallization^{9–11}. Crystallization times of the order of milliseconds in the highly oriented state are possible, compared to the order of minutes for crystallization under zero stress^{14,15}. Alten and Zachmann¹⁰ reported a decrease in the onset temperature for crystallization with increasing initial birefringence. Galli *et al.*¹⁶ revealed by means of infra-red spectroscopy and differential scanning calorimetry that chain segments of PET in the *trans* conformation begin to crystallize already below T_g . Nobbs *et al.*¹⁷ observed crystallization of oriented PET at low temperatures above 60°C. Therefore, thermally stimulated relaxation as well as crystallization of oriented chain segments will take place in nearly the same temperature range starting in the vicinity of T_g .

Oriented and glassy polymers exhibit a structural stability that is determined by the molecular mobility of chain elements and is therefore strongly dependent on both the temperature and the magnitude of internal stresses^{18,19}. Trznadel and Krzyszewski¹⁹ concluded that

* Present address: Eindhoven University of Technology, Department of Polymer Chemistry and Technology, PO Box 513, 5600 MB Eindhoven, The Netherlands

the appearance of shrinkage forces is mainly associated with the gradual relaxation of internal stresses frozen in the sample after deformation. Several authors^{2,17,19,20} demonstrated the sensitivity of shrinkage measurements to deformation conditions and thermal history. Pakula and Trznadel²¹ discussed the mechanism of generation of shrinkage forces by proposing a model to describe the shrinkage phenomenon.

Despite a large number of investigations, the temperature-dependent behaviour of highly oriented chains in the amorphous phase is not completely understood yet. The question arises as to how relaxation and crystallization processes affect each other with respect to temperature and microstructure.

Desai and Abhiraman¹³ pointed out several difficulties in the qualitative experimental and theoretical studies of the crystallization in oriented polymers due to a lack of information about: (a) the orientation distribution of uncrystallized chain segments, (b) orientation relaxation in the uncrystallized segments before and during crystallization and (c) crystallization-induced changes in the orientation distribution of uncrystallized chain segments during crystallization.

In this present study, non-crystalline PET structures with an extraordinarily large orientation of the molecular chains were prepared by means of uniaxial drawing procedures at temperatures below the glass transition (T_g). After that, they were annealed by using a step-by-step increase in the temperature. The resulting *in situ* changes of the supermolecular structure and the resulting thermomechanical behaviour of the drawn PET film strips have been investigated with respect to relaxation and crystallization processes.

PET is used as an ideal example for an oriented and glassy polymer. Contrary to other crystallization polymers, PET exhibits large half-times of crystallization, which enable chain orientation without crystallization. In addition, the high glass transition of about 70°C is far above room temperature and causes a freezing and easy treatment of oriented structures at room temperature. Using the model character of PET, the findings will result in new insights into the structure formation and deformation mechanism in crystallizable and flexible-chain polymers during drawing.

EXPERIMENTAL

Sample preparation

Nearly isotropic ($\Delta n \leq 0.005$) and X-ray amorphous PET film strips (sample 0) with a molecular weight of $M_w = 20\,000$, a thickness of 180 μm and a width of 2.8 mm were uniaxially drawn (Table 1). To avoid

crystallization, a drawing temperature (T_{dr}) of 20 and 68°C was used, which corresponds to a temperature below the glass temperature (T_g) of about 70°C. The drawing at $T_{dr} \leq T_g$, in the following denoted as cold drawing, is characterized by neck formation and propagation of the neck along the specimen. Two different drawing techniques, namely zone drawing (constant stress) and drawing in a homogeneous temperature field (constant drawing rate with necking) were applied to obtain the non-crystalline samples 1 and 8, respectively. In both cases, an extraordinarily large chain orientation was achieved (Table 1). The sample designation in Table 1 coincides with those in our previous investigations^{1,7,22,23}.

Differential scanning calorimetry

A Mettler DSC-30 was employed in the temperature range from -30 to 300°C using a heating rate of 5°C min⁻¹. The sample weight was about 10 mg.

Viscoelastic experiments

By means of a Rheometrics mechanical spectrometer (RMS-800), the temperature dependences of the storage modulus (E'), loss modulus (E'') and loss tangent ($\tan \delta = E''/E'$) were investigated. The drawn film strips (Table 1) with a sample length of about 20 mm were placed in a film shear attachment. The torsion movement at a frequency of $\omega = 10 \text{ rad s}^{-1}$ caused a mechanical loading along the sample drawing direction, and therefore a tensile modulus could be determined. The temperature was increased from -100 to 270°C at a rate of 3°C min⁻¹.

Wide-angle X-ray studies

Temperature-dependent X-ray experiments were performed by means of a Nicolet area detector together with an 18 kW rotating Cu-anode X-ray source (Rigaku RU-300)²³. The radiation beam was Ni-filtered and monochromatized. The samples were placed between two heating plates at a distance of 65 mm in front of the detector. The temperature was increased step by step and computer controlled to an accuracy of $\pm 0.5 \text{ K}$. WAXS experiments were carried out under vacuum of about 0.01 mbar at temperatures of 30, 50, 60, 70, 80, 90, 100, 120 and 160°C using a measuring time of 4 h after an annealing time of 2 h at each temperature. A small constant stress of 1.8 MPa was applied and therefore shrinkage could occur.

Using the Polymer beamline of HASYLAB at the DESY synchrotron facility in Hamburg, the time dependences of the scattering intensities of the equatorial WAXS reflections (010), ($\bar{1}$ 10) and (100) were

Table 1 Drawing conditions

Sample	Drawing temperature, T_{dr} (°C)	Neck propagation rate, v_{ne} (mm min ⁻¹)	Drawing stress, σ_{dr} (MPa)	Draw ratio, λ	Drawing method
1	68	18.2	15	4.3	zone drawing
8	23	30 (6% min ⁻¹)	neck propagation to λ_n^a	4.2	drawing in a homogeneous temperature field

^a Natural draw ratio

investigated. The experiments were performed at constant sample length, different annealing temperatures in the range from 50 to 240°C and under vacuum of about 0.07 mbar. The temperature was raised step by step from 20°C to the desired temperatures using a rate of 34°C min⁻¹. At each temperature, the intensity distribution along the equator was recorded immediately up to 2 h by accumulating a set of 30 s scans and employing a one-dimensional proportional counter with 512 channels and a resolution of 0.4 mm. The scattering angles are equivalent to the use of a Cu K_α beam. The data were corrected for the detector sensitivity and background scattering but not treated by any smoothing procedures.

Shrinkage experiments

The thermal shrinkage of PET samples has been studied by means of two methods providing the temperature dependence of the shrinkage strain as well as the shrinkage stress.

The shrinkage strain (S) was measured with an Instron apparatus in the temperature range from 25 to 120°C. During the experiment, a small constant stress of 1.8 MPa (comparable to WAXS) with an accuracy of the force $\Delta F = \pm 0.002$ N was applied. The large sample length of $l_0 = 500$ mm caused a high precision of the shrinkage strain. With regard to l_0 and l_i as the initial and the actual lengths, respectively, the shrinkage strain (S) was calculated from:

$$S (\%) = 100(l_i - l_0)/l_0 \quad (1)$$

The shrinkage stress (σ) and its time dependence were investigated at different temperatures by means of a Rheometrics mechanical spectrometer model 800. At each of the desired temperatures of 30, 50, 60, 80, 120 and 160°C, the rotation moment (ΔM) was measured in the time range from 0 to 7200 s (2 h). Then, the shrinkage stresses (σ) were calculated from the rotation moment (ΔM), radius ($r = 25$ mm) and cross-section (A) by using:

$$\sigma = \Delta M/(rA) \quad (2)$$

The sample length was chosen $l_0 = 20$ mm.

DISCUSSION

Initial material

The undrawn and initial PET sample 0 is non-crystalline according to WAXS and d.s.c. experiments and nearly isotropic with respect to birefringence measurements (Table 2). SAXS investigations have revealed no long period. From mechanical experiments, an elastic modulus of $E = 2$ GPa, a large viscoplastic deformation region ranging from 2.4 to 330% and a strain at break of about $\varepsilon_{br} = 400\%$ (Table 2) are determined. These values are known for non-crystalline and isotropic PET²⁴.

Birefringence and mechanical testing

The desired oriented samples 1 and 8 have been obtained by applying two different uniaxial cold-drawing procedures (Table 1) to the initial non-crystalline and isotropic PET film. Both samples are found to be X-ray amorphous with a large degree of chain orientation. Despite nearly the same draw ratio of $\lambda \approx 4.3$, differences in the microstructure as well as the resulting mechanical properties between samples 1 and 8 have been observed. According to birefringence (Δn) and elastic modulus (E), the chain orientation of sample 8 is larger than that of sample 1 (Table 2). The birefringences are measured to be $\Delta n = 0.200$ (sample 8) and 0.177 (sample 1). These are large values in comparison with $\Delta n_a = 0.275$ of a perfectly oriented amorphous PET phase²⁵.

Drawing has strongly changed the elastic modulus (E). According to static mechanical experiments¹, extraordinarily large values of $E = 8.4$ GPa for sample 1 and 10.2 GPa for sample 8 are obtained (Table 2). In this context, Padibjo and Ward²⁶ reported an excellent correlation between the modulus of drawn PET and the total contribution to the molecular orientation from *trans* conformers.

Moreover, the deformation behaviour of both drawn PET samples is characterized by a large plastic portion. Comparing samples 1 and 8, the higher strain limit for linearity (0.82% or 0.65%) and the larger strain at break (80% or 63%) together with smaller mechanical stresses at each strain value are related to a larger extensibility of the molecular network of sample 1¹.

Differential scanning calorimetry

The undrawn and initial PET sample 0 reveals a glass transition, crystallization and melting behaviour with the corresponding peak maxima at 68, 125 and 259°C, respectively (Figure 1 and Table 3). These values are known for non-crystalline and isotropic PET.

The comparison between the initial sample 0 and the drawn samples 1 and 8 (Figures 2 and 3) shows a significant shift of both the endothermal peak and the exothermal crystallization peak towards lower temperatures with increasing chain orientation.

In accordance with Trznadel *et al.*², the endothermal peak observed for oriented PET can be subjected to a combination of entropy and energy effects during thermal treatment. An increase in the temperature enables more extensive molecular motions associated with a relaxation of the locally stressed and constrained chains. This results in a more coiled conformation with a larger entropy. Furthermore, the endothermal behaviour reveals that energy dissipation should dominate over heat generation in that temperature region. Owing to the entropic and energetic processes above, the maximum of the endothermal peak of the oriented PET decreases by

Table 2 Sample characteristics

Sample	Birefringence, Δn	Elastic modulus, E (GPa)	Strain limit of linearity, ε_{lg} (%)	Strain at break, ε_{br} (%)
0	0.005	2.0	1.10	400
1	0.177	8.4	0.82	80
8	0.200	10.2	0.65	63

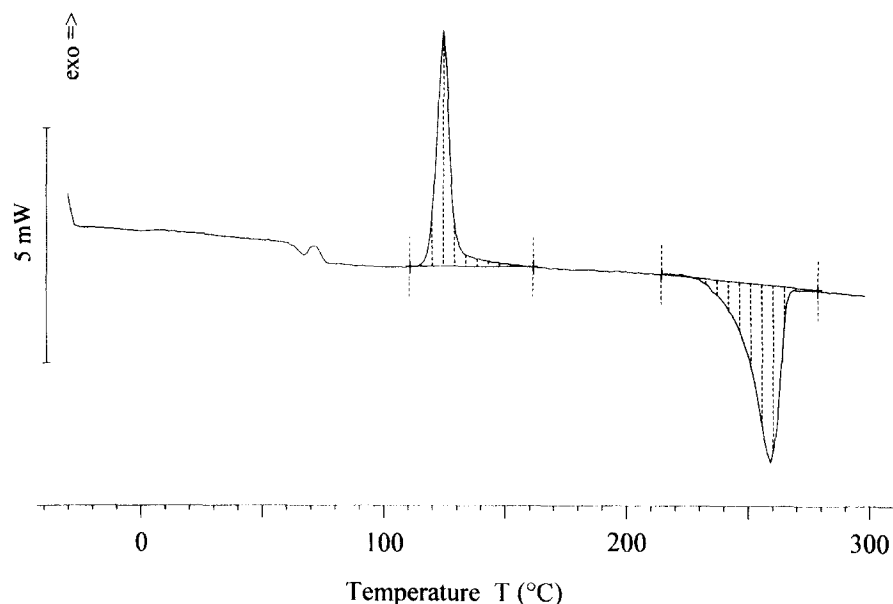


Figure 1 D.s.c. traces of the non-oriented and initial PET sample 0

7°C (sample 1) and 11°C (sample 8) in comparison to the undrawn sample 0 (Table 3).

The crystallization peak of the isotropic PET is very narrow (Figure 1) whereas the oriented samples (Figures

2 and 3) reveal a large temperature interval of crystallization. This is in agreement with the d.s.c. results from Trznadel *et al.*². Taking the maximum of the crystallization peak at $T_c \approx 79^\circ\text{C}$, a large decrease in the

Table 3 D.s.c. data

Sample	Endothermal peak, T (°C) (peak max.)	Crystallization peak		Melting peak	
		T_c (°C)	ΔH_c (J g ⁻¹)	T_m (°C)	ΔH_m (J g ⁻¹)
0	68	125	28.8	259	44.2
1	61	79	27.6	260	54.7
8	57	78	28.6	259	54.7

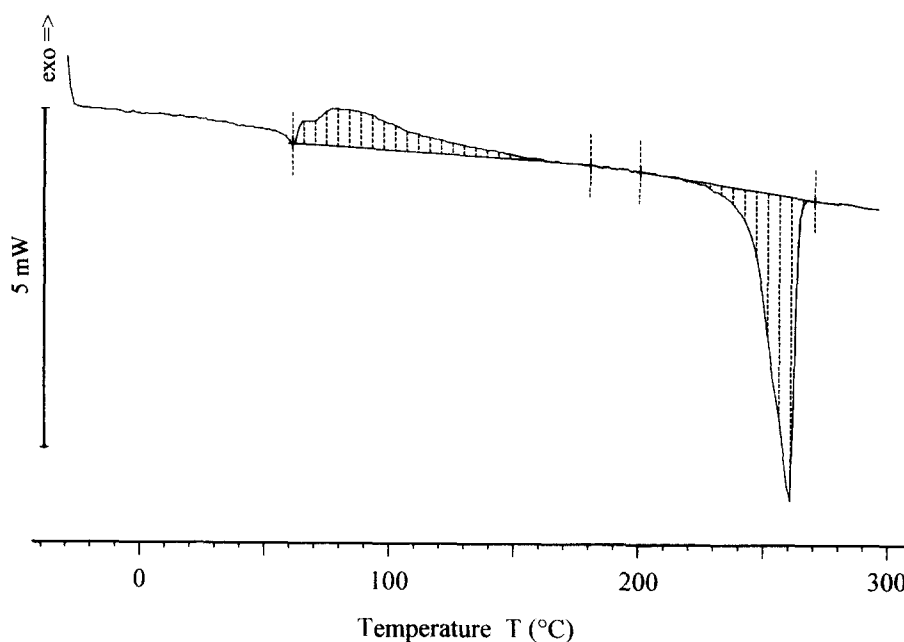


Figure 2 D.s.c. traces of the oriented PET sample 1

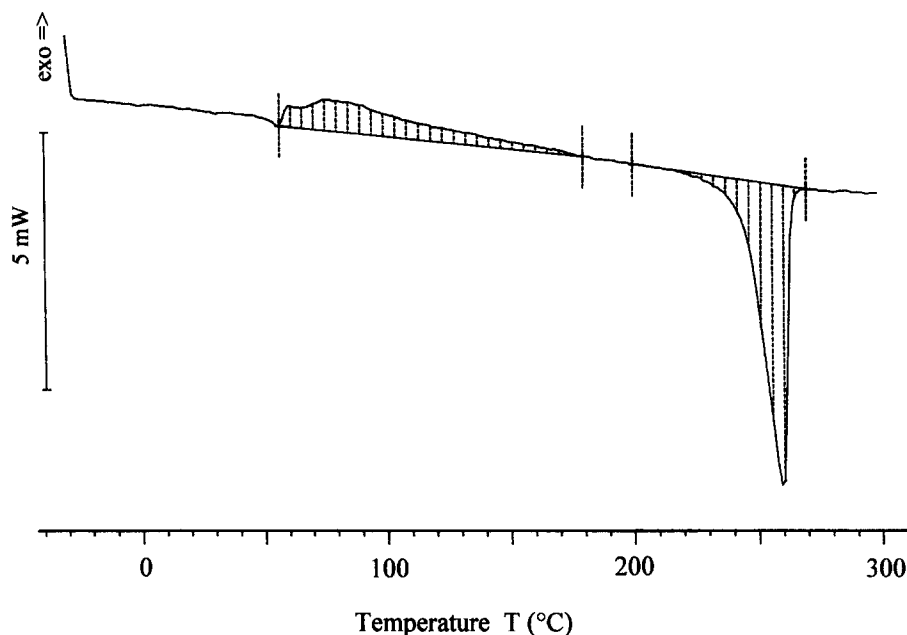


Figure 3 D.s.c. traces of the oriented PET sample 8

crystallization temperature by about 46°C with cold drawing is found (Table 3). The onset temperature for crystallization is ascertained at temperatures as low as 56°C (sample 8) and 62°C (sample 1). From the total area under the exothermal d.s.c. peak, a crystallization enthalpy of $\Delta H_c \approx 28 \text{ J g}^{-1}$ is determined for the isotropic and initial sample 0 as well as the oriented samples 1 and 8. The corresponding mass crystallinity (χ) can be calculated to be about 24% by means of the equation:

$$\chi_{\text{dsc}} = \Delta H_{\text{exp}} / \Delta H_{\text{mc}}^* \quad (3)$$

where ΔH_{exp} can be either the experimentally determined crystallization or melting enthalpy and $\Delta H_{\text{mc}}^* = 28.1 \text{ cal g}^{-1}$ (ref. 27), equal to 117.6 J g^{-1} , characterizes the melting enthalpy of fully crystalline PET.

Drawing has not affected the melting temperature (T_m), which remains unchanged at $T_m \approx 260^\circ\text{C}$ (Table 3). Contrary to that, the melting enthalpy of PET increases with drawing from $\Delta H_m = 44.2$ to 54.7 J g^{-1} . Using equation (3), these findings correlate with a smaller mass crystallinity of $\chi \approx 38\%$ for the isotropic sample 0 compared to $\chi \approx 47\%$ for the oriented samples 1 and 8.

Viscoelastic experiments

As is known, dynamic mechanical thermal analysis (d.m.t.a.) on PET reveals only one loss modulus (E'') peak in the range from room temperature to the melting point at about 265°C. The corresponding dispersion is due to the glass transition. The maximum of the E'' peak measured at a sinusoidal strain with the frequency of 110 Hz can shift from about 80°C for non-oriented and non-crystalline PET²⁴ to about 150°C with increasing chain orientation and molecular order²².

In the case of the highly oriented and non-crystalline samples 1 and 8, two maxima of the loss modulus (E'')–temperature curve have been found at 80 and 127°C (Figures 4 and 5). The peak at 80°C corresponds to the

glass transition of wholly non-crystalline PET without any hindrance in the molecular mobility. The second maximum in E'' at 127°C can be related to the glass transition of the oriented and non-crystalline phase with a limited molecular mobility.

Owing to the larger chain orientation in the case of sample 8, the peak intensity at 80°C is smaller for sample 8 than that for sample 1. The measured increase in the storage modulus (E') close to 80°C cannot be explained by relaxation processes. In general, the material stiffness and therefore E' decreases in each dispersion region. Contrary to that, crystallization would strengthen the molecular network and consequently cause an increase in E' . The occurrence of crystallization in that temperature region is confirmed by d.s.c. experiments.

Two-dimensional wide-angle X-ray scattering experiments

Two-dimensional WAXS experiments have been performed at different temperatures after an annealing time of about 2 h. The oriented and glassy PET structures are loaded by a small stress, which gives the possibility for free shrinkage. In the following, the structural changes with temperature will be demonstrated from sample 1. The WAXS patterns of sample 8 are similar to those of sample 1.

As is seen from WAXS investigations, low annealing temperatures in the range from 30 to 60°C do not affect the microstructure of the drawn samples 1 and 8. There is only the amorphous peak along the equator without any changes of the peak position and intensity with temperature.

A first reorganization of the structure is seen at 70°C (Figures 6 and 7). The intensity of the amorphous peak has increased slightly and a starting deformation of the WAXS pattern is noticed. Under the annealing condition at 70°C, the formation of the non-equatorial crystalline reflections (0 1 1), (1 1 1) and one close to the (0 1 1) and (1 1 1) has taken place. These changes are due to crystallization. Consequently, the onset temperature for

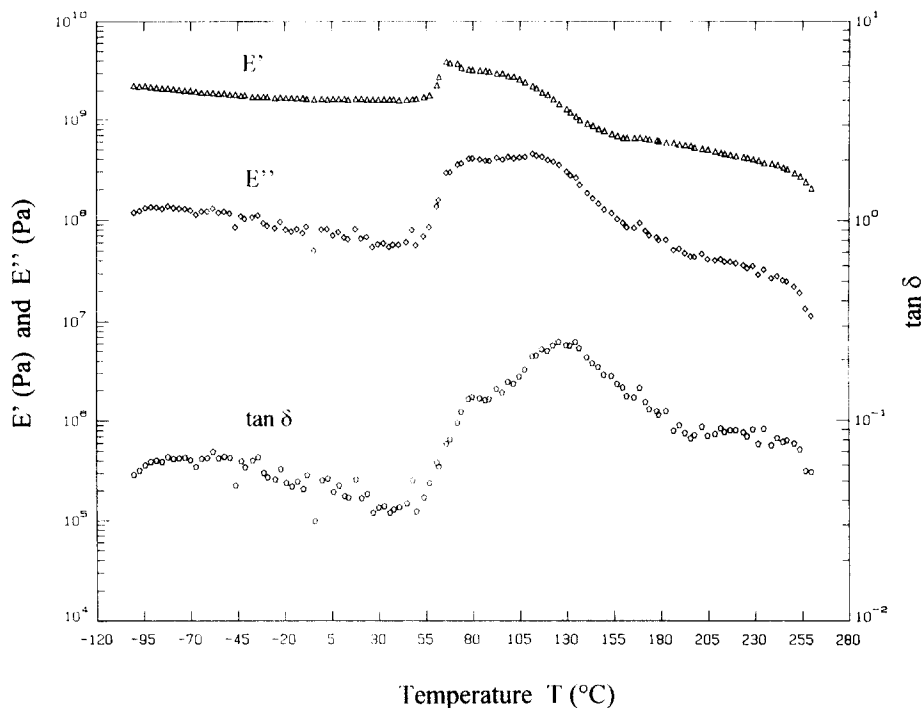


Figure 4 Temperature dependence of the storage modulus (E'), loss modulus (E'') and loss tangent ($\tan \delta$) of the oriented PET sample 1

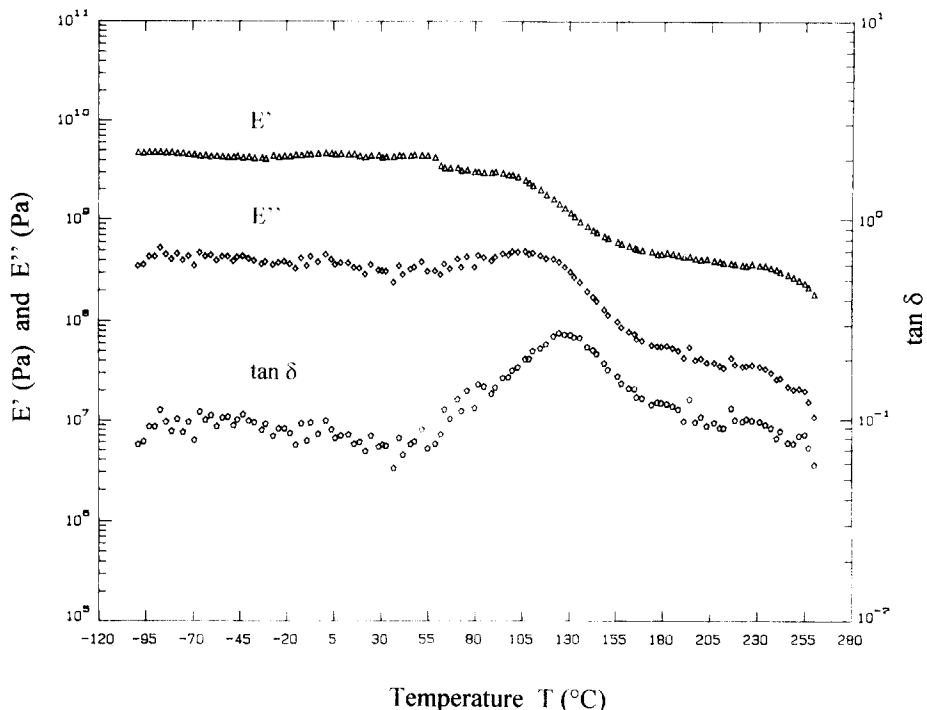


Figure 5 Temperature dependence of the storage modulus (E'), loss modulus (E'') and loss tangent ($\tan \delta$) of the oriented PET sample 8

crystallization of highly oriented PET structures is much lower than the corresponding temperature in the vicinity of 90°C for isotropic PET. This is in agreement with refs 10, 16 and 17. The patterns reveal a dominant formation of the non-equatorial ($hk1$) reflections at low annealing temperatures contrary to almost no changes in the equatorial intensity distribution.

With increasing temperature, the molecular order improves step by step. Next, the formation of the ($\bar{1}12$) reflections has started at 80°C (Figures 6 and 7).

The crystalline PET structure is still disturbed at 90°C, which is in agreement with Fischer and Fakirov²⁸. As is seen in Figures 6 and 7, the three (010), ($\bar{1}10$) and (100) crystalline reflections along the equator start to grow. These reflections characterize three planes of the triclinic unit cell, which are aligned into the drawing direction (z)²⁹. For highly oriented PET, the very small angles between these planes and the drawing direction were discussed in a previous paper²³.

At 120°C, a well-developed crystalline structure is

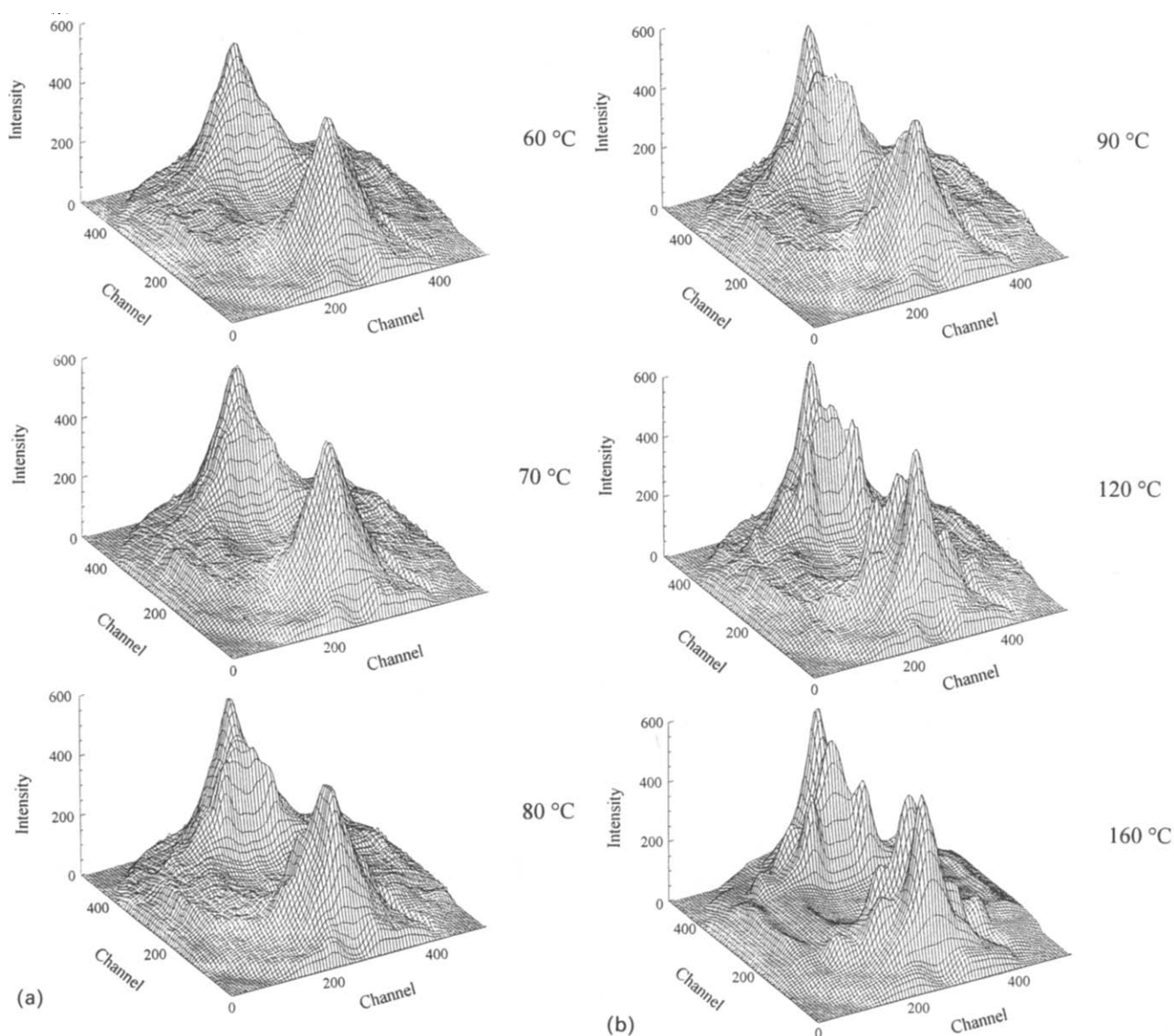


Figure 6 WAXS intensity plots of the oriented PET sample 1 at different annealing temperatures. The incident beam is chosen perpendicular to the film plane. The drawing direction lies vertical in the figure. The number of channels is equal to the scattering angles

found. With further increase in the annealing temperature, the molecular order has been improved at 160°C.

Synchrotron wide-angle X-ray scattering experiments

WAXS synchrotron studies on samples 1 and 8 in the temperature range from 50 to 240°C under constant sample length have revealed crystallization of the oriented PET structures with increasing annealing temperature above 80°C. With respect to the equatorial crystalline reflections (010), ($\bar{1}$ 10) and (100), a significant temperature-dependent formation is observed. After reaching the desired annealing temperatures, almost no changes of the equatorial integrations with time are found. The largest effects are still seen for the highest annealing temperature of 240°C, as represented for sample 8 in Figure 8. Consequently, structural changes take place mainly during the heating period and they are almost completed within less than 7.5 min. These findings underline, in agreement with refs 9–11, 14 and 15, the fact that highly oriented PET structures crystallize very fast, even at comparably low temperatures such as 120°C. Furthermore, it can be concluded

that the temperature regime used for the two-dimensional WAXS experiments is appropriate to investigate quasi-static structures.

Shrinkage strain experiments

The shrinkage strain (S) of the drawn sample 1 is zero in the temperature range from 25 to 50°C (Figure 9). With a further increase in the temperature, S increases strongly. This is due to a rise in the molecular mobility with temperature, which enables conformational changes. The shrinkage strain reaches 5.5% and 7.7% at 100°C and 120°C, respectively. A comparable shrinkage behaviour to that of sample 1 is found for sample 8.

As is seen in Figure 9, the shrinkage strain–temperature curve reveals a turning point at about 70°C. That point is related to the beginning of the crystallization process. Crystallization decreases the differential coefficient dS/dT with temperature (T). D.s.c. and WAXS experiments have confirmed the occurrence of crystallization at the temperature above.

The cooling of sample 1 from 100 down to 30°C does not affect the shrinkage strain. S also remains unchanged

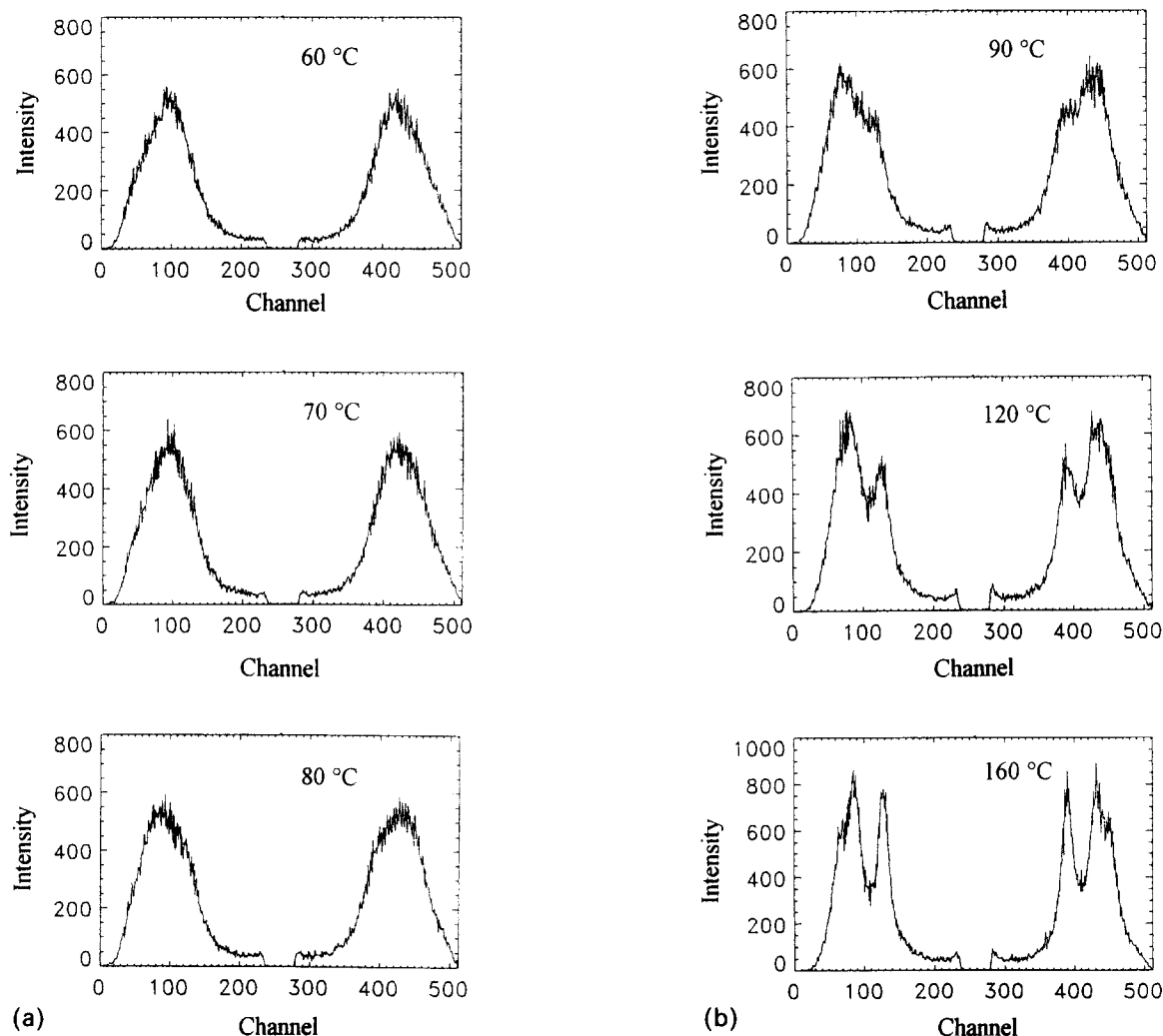


Figure 7 WAXS equatorial integrations of the oriented PET sample 1 at different annealing temperatures. The incident beam is chosen perpendicular to the film plane. The drawing direction lies vertical in the figure. The number of channels is equal to the scattering angles

during a later temperature increase up to the previous temperature of 100°C. Such behaviour is subjected to a freezing of the shrinkage in relation to a decrease in the chain mobility. Bonart *et al.*²⁰ already reported a thermally stimulated reversible change of the shrinkage strain up to the previous annealing temperature for cold-drawn polycarbonate with a draw ratio of 1.6.

Shrinkage stress experiments

The oriented samples 1 and 8 have revealed no shrinkage in the temperature range from 30 to 50°C, which is due to frozen-in configurations. The shrinkage stress (σ) is close to zero and remains nearly unchanged within the investigation time of 2 h. Because of similar results for samples 1 and 8, the shrinkage behaviour will be discussed by means of *Figure 10* for sample 1.

Immediately after reaching 60°C, a large increase in the shrinkage stress is observed. It can be assumed that the extended molecular chains undergo thermally activated transitions from their oriented into unoriented states. Such relaxation processes are influenced by internal stresses exerted by the extended macromolecules on the local frozen-in configurations³⁰. The resulting state is of intermediate character. The relaxation of the local molecular orientation affects the transfer of the initially frozen-in internal stresses to the surrounding

matrix³⁰. With respect to *Figure 10*, the shrinkage stress (σ) at 60°C has reached a plateau value after 2 h. A similar time-dependent behaviour with a fast stress rise of σ in the short-time range and a slower increase at longer times was reported by Trznadel¹⁸ for oriented and glassy polycarbonate and poly(ethylene terephthalate).

Starting from 60°C, a temperature rise towards 80, 120 and 160°C produced immediately a large decrease in the shrinkage stress in order to tap the appropriate stress level for each temperature (*Figure 10*). As is known from d.s.c. and WAXS experiments on the drawn samples 1 and 8, crystallization can occur already at low temperatures in the vicinity of 60°C. Therefore, relaxation and crystallization processes have to be taken into account to describe the shrinkage behaviour of oriented and initially glassy PET. According to Trznadel and Kryszewski¹⁹, crystallization stabilizes the structure due to the cross-linking effects of growing crystallites. Consequently, crystallization would decrease the shrinkage stress.

The change of the shrinkage stress with each temperature step in the range from 60 to 160°C is mainly affected by a superposition of orientation and crystallization processes. The shrinkage stress decreases at a rate of 0.065 MPa K⁻¹ during the temperature rise from 60 to 80°C, which is much larger than 0.025 MPa K⁻¹ for the increase from 80 to 120°C and

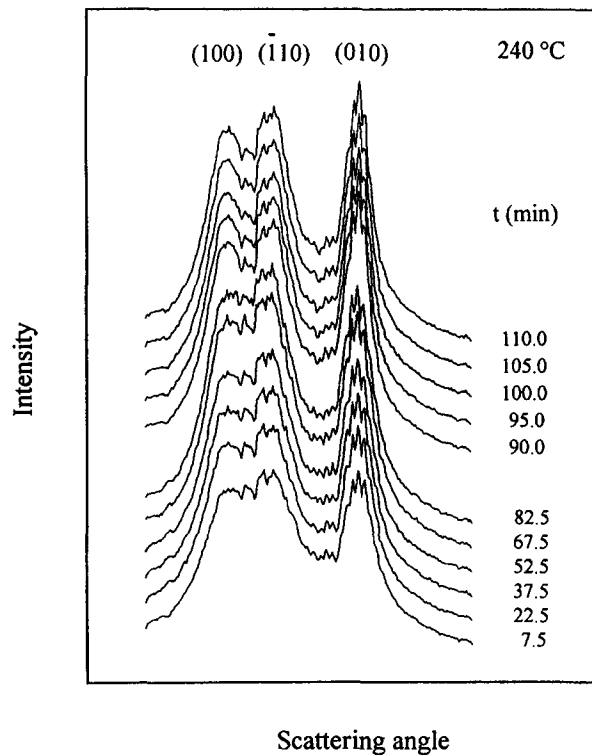


Figure 8 Change of the synchrotron WAXS scattering intensities with total time (t) by accumulating a set of 30 s scans during annealing at 240°C of the oriented PET sample 8. The time range to reach the desired temperatures is omitted. Represented are the intensity distribution along the equator. The incident beam is chosen perpendicular to the film plane. The drawing direction lies vertical in the figure

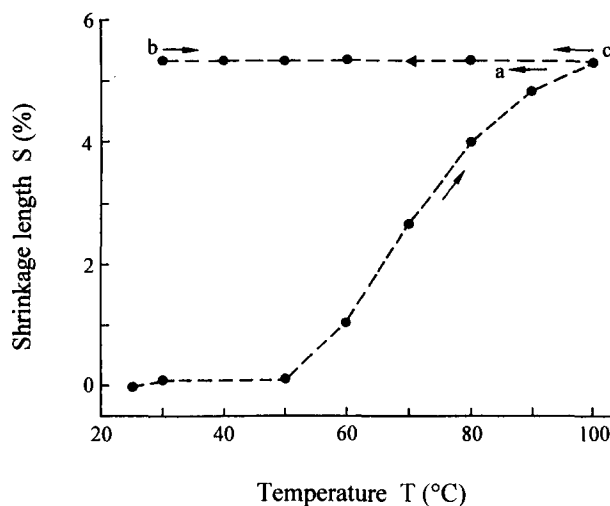


Figure 9 Temperature dependence of the shrinkage strain (S) of the oriented PET sample 1. The reversibility of S is shown by (a) a cooling from 100°C followed by (b) a heating from 60°C and (c) a second cooling from 100°C

almost comparable to 0.06 MPa K^{-1} for 120 to 160°C. It can be concluded that each temperature step initiates a further crystallization, which counteracts internal stress relaxation. The large σ decrease in the temperature ranges from 60 to 80°C and 120 to 160°C is probably due to a dominant crystallization effect.

The time dependence of the shrinkage stress at each temperature step provides further information about the time constants of the underlying structural changes. According to Figure 10, the shrinkage stresses (σ) at 60 and 80°C reach a plateau value within the investigation time of 2 h. With increasing annealing temperature from 80 to 160°C, σ becomes slightly time-dependent. In this temperature range, relaxation and crystallization pro-

cesses are very fast. Relaxation experiments on sample 1 in a previous paper²² revealed $E(t)$ modulus changes at $T = 120^\circ\text{C}$ in a time range of $t < 5$ s, whereas $E(t)$ was found to be almost time-independent in the range from 5 to 1000 s. Thompson¹⁴ and Smith and Steward¹⁵ both reported extremely short crystallization times of the order of milliseconds for highly oriented structures. Therefore, the long-time decrease in the shrinkage stress observed in the time range from 30 to 120 min should be subjected to an intermolecular slippage of stressed chain segments. Additional intramolecular slippage may also be possible at higher temperatures but the normal stress applied during the experiment was only small.

Cooling from 160 down to 30°C immediately causes a

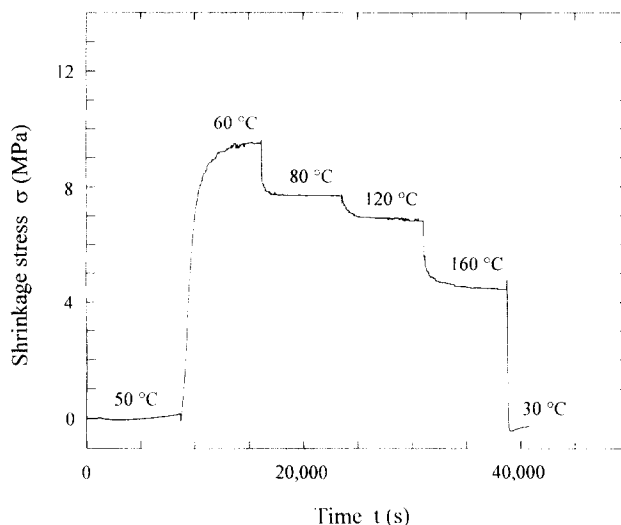


Figure 10 Time dependence of the shrinkage stress (σ) of the oriented PET sample 1 at different temperatures

large decrease in the shrinkage stress (σ) towards a value close to zero (Figure 10). The reversibility of σ reveals that irreversible deformations, which can occur at higher temperatures, are negligible.

CONCLUSIONS

Two different cold-drawing procedures with well-defined parameters were applied to prepare highly oriented and glassy PET structures from isotropic and X-ray amorphous initial film strips. Drawing at a draw ratio of about 4.3 caused PET samples 1 and 8 with large elastic moduli of 8.4 and 10.2 GPa and birefringences of 0.177 and 0.200, respectively.

Calorimetric (d.s.c.) studies have revealed onset temperatures for crystallization as low as 56°C (sample 8) and 62°C (sample 1). With drawing, a decrease in the maximum of the crystallization peak from 120 to 79°C and an increase in the melting enthalpy from 44.2 to 54.7 J g⁻¹ is found. However, the melting temperature remains unchanged at about 260°C.

Dynamic mechanical thermal analysis (d.m.t.a.) has shown two maxima of the loss modulus-temperature curve at 80 and 127°C, which corresponds to the glass transition of the non-crystalline phase without and with a limited molecular mobility, respectively. The increase in the storage modulus close to 80°C cannot be explained by relaxation processes. Such an increase is due to crystallization.

In situ two-dimensional wide-angle X-ray (WAXS) studies have described the step-by-step formation of the crystalline molecular order with temperature. It is remarkable that crystallization takes place with the formation of the non-equatorial (0 $\bar{1}$ 1), ($\bar{1}$ 11) and one close to the (011) and (1 $\bar{1}$ 1) reflections at 70°C, the formation of the ($\bar{1}$ 12) reflections at 80°C and, finally, the formation of the equatorial (010), ($\bar{1}$ 10) and (100) reflections at 90°C. The equatorial reflections characterize the three planes of the triclinic unit cell aligned into the drawing direction. The crystal formation, which only takes place at higher temperatures, underlines the existence of a disturbed molecular order at low crystallization temperatures.

Synchrotron WAXS investigations with respect to the equatorial reflections (010), ($\bar{1}$ 10) and (100) have shown a fast crystallization process. The final crystal structure for each temperature above 120°C is reached within less than 7.5 min.

Shrinkage strain and stress experiments have revealed both the relaxation of local molecular orientation starting at about 50°C and the onset temperature for crystallization of about 70°C. The superposition of the two effects above with temperature has been analysed in detail.

REFERENCES

- Göschel, U. *Acta Polym.* 1989, **40**, 23
- Trznadel, M., Pakula, T. and Kryszewski, M. *Polymer* 1988, **29**, 619
- Pakula, T. and Fischer, E. W. *J. Polym. Sci., Polym. Phys. Edn.* 1981, **19**, 1705
- Zachmann, H. G. *Polym. Eng. Sci.* 1979, **19**, 966
- Cavrot, J. P. and Rietsch, F. *Eur. Polym. J.* 1985, **21**, 787
- Andrianova, G. P., Popov, Ju. V. and Artamonova, S. D. *Vysokomol. Soedin. (B)* 1975 **17**, 876
- Hofmann, D., Göschel, U., Walenta, E., Geiss, D. and Philipp, B. *Polymer* 1989, **30**, 242
- Biangardi, H. J. and Zachmann, H. G. *J. Polym. Sci., Polym. Symp.* 1977, **58**, 169
- Le Bourvellec, G., Monnerie, L. and Jarry, J. P. *Polymer* 1987, **28**, 1712
- Alten, G. and Zachmann, H. G. *Makromol. Chem.* 1979, **180**, 2723
- Sawatari, C. and Matsuo, M. *Textile Res. J.* 1985, **55**, 547
- Quian, R., He, J. and Shen, D. *Polym. J.* 1987, **19**, 461
- Desai, P. and Abhiraman, A. S. *J. Polym. Sci., Polym. Phys. Edn.* 1985, **23**, 653
- Thompson, A. B. *J. Polym. Sci.* 1959, **XXXIV**, 741
- Smith, F. and Steward, R. D. *Polymer* 1974, **15**, 283
- Galli, R., Canetti, M., Sadocco, P., Seves, A. and Vicini, L. *J. Polym. Sci., Polym. Phys. Edn.* 1983, **21**, 717
- Nobbs, J. H., Bower, D. I. and Ward, I. M. *Polymer* 1976, **17**, 25
- Trznadel, M. *Polymer* 1986, **27**, 871
- Trznadel, M. and Kryszewski, M. *Polymer* 1988, **29**, 418
- Bonart, R., Fenzl, M. and Schmidt, K. *Acta Polym.* 1987, **38**, 281
- Pakula, T. and Trznadel, M. *Polymer* 1985, **26**, 1011
- Göschel, U. *Polymer* 1992, **33**, 1881
- Göschel, U., Deutscher, K. and Abetz, V. *Polymer*, 1996, **37**, 1
- Göschel, U. and Nitzsche, K. *Acta Polym.* 1985, **36**, 580
- Dumbleton, J. H. *Polym. Sci (A-2)* 1968, **6**, 795

- 26 Padibjo, S. R. and Ward, I. M. *Polymer* 1983, **24**, 1103
- 27 Miyagi, A. and Wunderlich, B. *J. Polym. Sci., Polym. Phys. Edn.* 1972, **1**, 2085
- 28 Fischer, E. W. and Fakirov, S. *J. Mater. Sci.* 1976, **11**, 1041
- 29 Daubeny, R. de P., Bunn, C. W. and Brown, C. J. *Proc. R. Soc. (Lond.) (A)* 1954, **226**, 531
- 30 Trznadel, M., Pakula, T. and Kryszewski, M. *Polymer* 1985, **26**, 1019